Environ. Eng. Res. 2024; 29(1): 220758
https://doi.org/10.4491/eer.2022.758

pISSN 1226-1025
eISSN 2005-968X

Research

Investigation of the aerosol's optical properties over the dust prevalent semi-arid region at Jaipur, northwestern India

Ranjitkumar Solanki†, Kamlesh Pathak

Department of Physics, Sardar Vallabhbhai National Institute of Technology, Surat-395007, India

Received December 17, 2022 **Revised** April 18, 2023 **Accepted** April 21, 2023

ABSTRACT

Jaipur is a key site to study Aerosol Optical Depth (AOD) due to unpredictable variation of atmospheric Aerosols particles in the recent years. Aerosols Optical Depth (AOD) and Angstrom Exponent (AE) were investigated over the semi-arid region, Jaipur (26.9124° N, 75.7873° E) Northwestern India during the April-2009 to December-2017 utilizing AERONET CIMEL sun-photometer level-2 data for aerosols spatial and temporal characteristics. The Aerosols Optical Depth AOD_{500} nm, AOD_{440} nm, and AOD_{340} nm were observed maximum in July-2011 and minimum observed in March-2013. The monthly mean Angstrom Exponent (AE) was maximum (1.53 ± 0.43) for 500-870 nm, (1.49 ± 0.4) for 440-870 nm, and (1.19 ± 0.32) for 340-440 nm in September 2011, while the lowest value recorded (0.26 ± 0.12) for 340-440 nm, (0.16 ± 0.08) for 440-870 nm and (0.15 ± 0.07) for 500-870 nm during June 2014. The backward trajectories analysis was performed using the Hybrid Single-Particle Lagrangian Integrated Trajectories (HYSPLIT) model to determine the sources of large aerosol loadings over the Jaipur region, and air mass simulations from the back trajectory, suggest that the Thar desert northwestern part of India is the source of highest aerosols dust particle over the study area during the pre-monsoon season.

Keywords: AERONET, AOD, HYSPLIT, Jaipur

Graphical Abstract

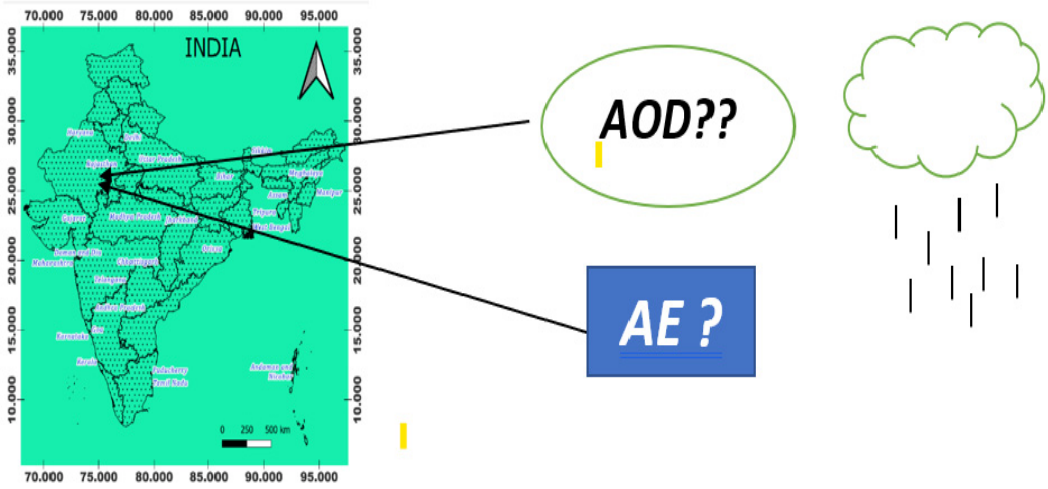

† Corresponding author
E-mail: ranjit33solanki@gmail.com
Tel: +917984808748
ORCID: 0000-0001-9348-0362

1. Introduction

Aerosol is a multi-phase system consisting of solid or liquid particles suspended in the atmosphere. An aerosol is a crucial component of atmosphere, directly impacting the Earth's atmospheric system by absorbing and scattering solar radiation and helps to maintain energy budget by absorbing and scattering solar radiation. However, it also has an indirect or semi-direct impact on the regional and global atmospheric environment, human health, and visibility [1-4]. Aerosols have significant climatic and environmental consequences around the globe. The impacts of aerosol optical characteristics on the Earth's climate have been significantly studied [5]. Certain meteorological parameters as Temperature (T), Relative Humidity (RH), and Wind Speed (WS) cause significant variation on the optical characteristics of aerosols.

Aerosol optical characteristics are exclusively investigated due to its large impact on global climate and plays significant role in atmospheric forecast [6–9]. Ground-based and satellite remote sensing are two primary approaches to measuring atmospheric aerosols. To evaluate the optical characteristics of aerosols, long-term ground-based monitoring is the essential [10-15]. For ground-based measurement, the AERONET network is used to investigate the properties of aerosols [16]. The ground-based radiometric observations over south Asia provided an insight into the strong seasonal variation of aerosol loading. Also, the changes in aerosol properties over the Indo Gangetic Plains (IGP) over India can be observed by in situ approach [17-28].

IGP is a significant area for aerosol study due to their impact on the Earth's atmosphere. The Thar Desert is the primary source of aerosols in the east, while the highly populated industrial area is in situated at the west. Many abiding research demonstrates that radiative impacts of the aerosol during high pollution episodes [29, 30]. Mineral dust and other anthropogenic carbonaceous and sulfate aerosol components have been added to the pre-monsoon aerosol load. Western Indian region shows frequent dust storms yearly during the pre-monsoon season (April to June). Due to significant aerosol loading in the pre-monsoon and early monsoon, Western Indian region is strongly impacted by frequent and intense dust storms. This may lead to an impact on monsoon activity over the IGP region drastically [23, 31]. It is vital to characterize the aerosol characteristics above Jaipur in north-west India because it is close to the Thar desert, a significant source of dust for both Asia and India. Systematic investigation over Jaipur region was primarily concerned for the seasonal fluctuations in aerosol characteristics under specific occurrences, such as dust transport, industrial pollution, domestic activities, etc. [32, 33]. Long-term observation of aerosol characteristics in as numerous locations as feasible all over India is needed to produce representative observations and a greater sense of such vast occurrences.

A review of observational and modeling research over South Asia also sheds light on the Asian pollution outflow and its large-scale consequences [34]. Mineral dust is one of the principal natural aerosol species over the Continental Tropical Convergence Zone (CTCZ) region during spring and summer. The dust is transported by winds and convective motion over large dry regions as well as deserts of western Asia and Eastern Africa [35, 36]. During the pre-monsoon season over the Gangetic basin in India, remote sensing data revealed high aerosol loading due to dust effect [18-35]. The Thar Desert, located in northwestern India (440-500 km from Jaipur) and eastern Pakistan, is one of the most essential dust-producing areas on the Indian subcontinent [38-40]. Jaipur the capital state of Rajasthan India, by its geographical and climatological condition in northwestern India near Thar Desert, is a key site for investigation of Aerosol Optical Depth (AOD) due to unpredictable variation of atmospheric Aerosols particles in the recent years. It experiences seasonal dust storms every year. Dust storms are widespread and play a profound impact on the climate area.

Additionally, the radiative effects of Aerosol over northern India and the foothills and slopes of the Himalayas are a possible source of aerosol–monsoon climate disruption [41-44]. The Aerosol activity at the IGP region is considerably affected by burning of crops every year, primarily in the post-monsoon season over Punjab, Haryana, and western Uttar Pradesh regions. These regions are known as India's "bread basket" since they generate over two-thirds of the country's food grains [45-47]. Several studies have consistently reported the rise in aerosol loading during two seasons (pre-monsoon and post-monsoon seasons) in the IGP region. The major cause of the increment in observed aerosol may be the different pollution sources like dust and biomass burning [18, 21, 30, 48-54]. Hence, the considerable trends in AOD (Aerosol Optical Depth) are not yet analyzed. In order to understand the long-term trends between the atmospheric parameters, a consistent study over Jaipur region is essential.

Aerosol optical depth (AOD) is a measure of the degree up to which the aerosols prevent solar radiation. It is also known as Aerosol Optical Thickness (AOT) and is defined as integrated extinction coefficient over a vertical column of atmosphere of unit cross section. The phenomena such as dust storms, forest fires and biomass burning can be monitored utilizing the distribution of this parameter. It is an exponent expressing the spectral dependence of aerosol optical depth with wavelength of the incident light. Angstrom exponent is often used to indicate the size of the aerosol particles. The values greater than two represent small particles associated with combustion by products and values less than one indicating large particles like sea-salt and dust. It also gives information on the aerosol phase function and the relative magnitude of aerosol radiances at different wavelengths. The parameter is applied in characterization of aerosol types, Earth radiation budget study, radiation transfer models etc. A number of investigations have been noticed during last two decade that the aerosols along with their impact on environmental quality and local climate [48-53] Aerosol optical depth (AOD) estimation at various wavelength is curtail, easier and suitable parameters for aerosol characteristics. Angstrom Exponent AE is also key indicator of the foremost size [54-56] due to its spectral shape of the extinction is related to the particle size.

The present study consists of the AERONET sun-photometer data to depict fluctuations in aerosol optical characteristics on annual and seasonal time scales during the study periods (2009-2017). This study investigated regional aerosol properties and origins using the AERONET data and air mass back trajectory

(HYSPLIT). Backward trajectories analysis was performed using the Hybrid Single-Particle Lagrangian Integrated Trajectories (HYSPLIT) model which is the most widely used atmospheric transport and dispersion models in the atmospheric research community, to determine the sources of significant high aerosol loadings over Jaipur region during the study period. According to Wang *et al.*, the HYSPLIT model is an effective tool for understanding dust emission, transport, and deposition and complementary for analyzing and interpreting ground-based and satellite-based observations [57].

2. Site Description and Data Collection

2.1. Synoptic Meteorology and Method

The Jaipur site (26.91 °N, 75.78 °E) is on the eastern edge of the Thar Desert, flanked on three sides by the Aravalli Mountains [33,58,59]. It is India's most populous city having 3.1 million populations. Jaipur is known for its tropical and semi-arid environment throughout the year. Additionally, it is surrounded by hills to the north and east and is located at 431 m AMSL (Above Mean Sea Level). Jaipur consists of many small-scale industries such as engineering, metals, wood, transport, paper and leather, textile, chemical and petroleum, food, etc. which are forming clusters in the west and south regions of the city. During the pre-monsoon (April-May) season, severe dust storms and sandstorms occur in Jaipur region [57]. During the monsoon (July–August), winds from the eastern half of the Ganga River basin transport precipitation, as well as the Thar Desert deliver regular dust storms and create a dry climate. The entire area is dominated by aerosols from anthropogenic sources accumulated by local and northerly winds during the post-monsoon (September–October) and winter (November–February) seasons [57].

The ambient meteorological parameters obtained from the NASA Langley Research Center (LaRC) POWER Project, Web service (https://power.larc.nasa.gov/) for April-2009 to December-2017 show a distinct seasonal pattern of weather. Temperature and Relative Humidity (RH) were incorporated into the study to determine how the various properties of aerosol (AOD-Aerosol Optical Depth and AE-Angstrom Exponent) are dominantly affected by variation in these parameters. The temperature data was downloaded in K (Kelvin) and then converted to ℃ for proper association with Relative Humidity and optical characteristics (AOD and AE).

Fig. 1 depicts the meteorological parameters over the study region during the study period (April-2009 to December-2017). During the pre-monsoon months of April to May, the average monthly temperature ranges from 31℃ to 37℃ (Fig. 1(A)). However, the average maximum temperature was 39℃ in June 2014(Fig.

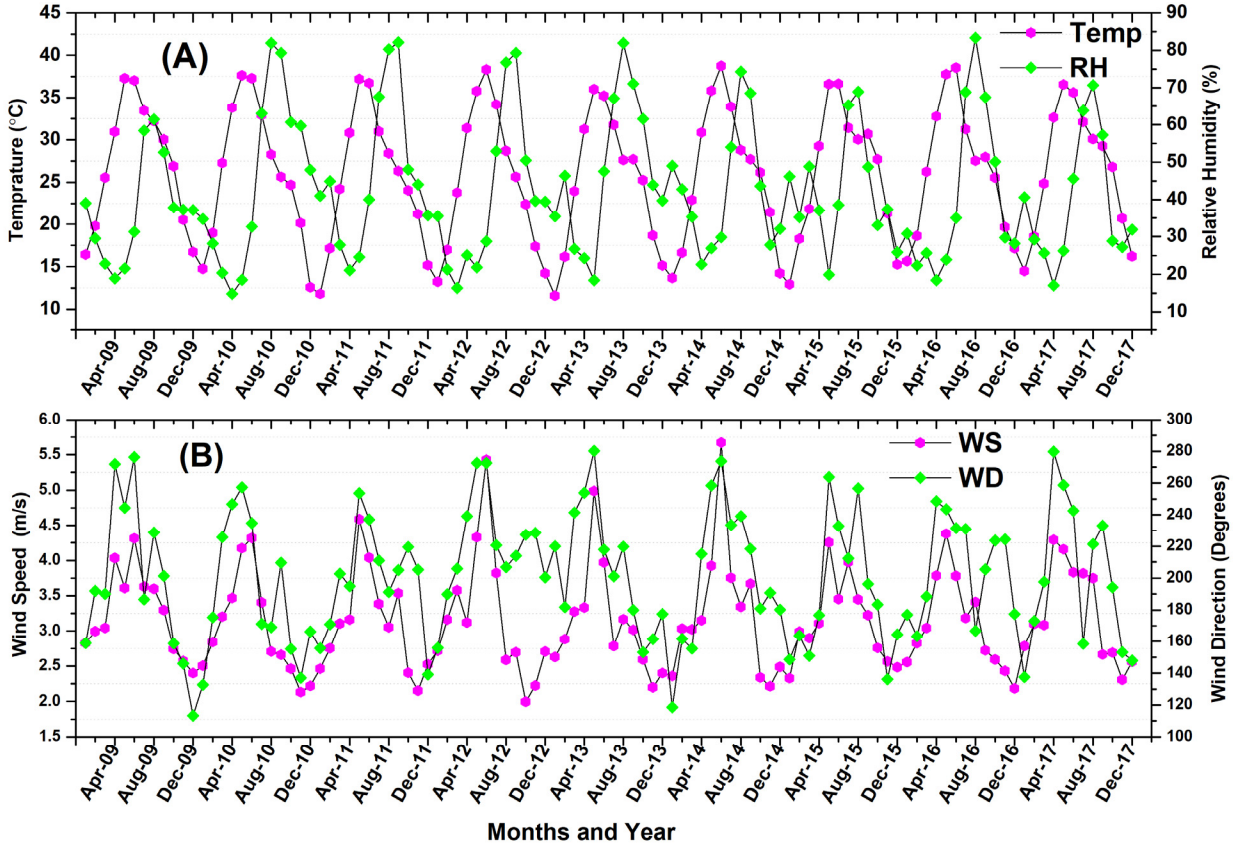

Fig. 1. (A) Averaged monthly temperature (°C), relative humidity (%), and (B) Averaged monthly wind speed (m/s), and wind direction (degree) over study location.

1(A)). The average temperature in the pre-monsoon (April-May) is 35℃ varies from 2 to 3℃, and in the winter (December-March), it is 5 to 15℃ with medium rainfall (60 cm) (Fig. 1(A)). August 2016 had the highest average Relative Humidity (RH) of 85%, and shows high humidity in August-2010, 2011 and August-2013 (during the rainy season) near about 82-84 (Fig. 1(A)). Relative humidity exhibits two peaks during the monsoon and the other in January (in winter) (Fig. 1(A)). Due to the considerable diurnal change in temperature, the most remarkable difference between the maximum and minimum Relative Humidity (RH) occurred during the pre-monsoon season. Wind speeds usually follow the temperature trend over the location. The predominant wind direction is between 200 and 230 degrees (southwest) during May and June (Fig. 1(B)).

2.2. AErosol Robotics NETwork (AERONET) AOD Data

The ground-based observation was utilized in this study to evaluate aerosol variability for the Jaipur stations throughout a study period (April 2009 – December 2017) from the AERONET AOD (https://aeronet.gsfc.nasa.gov/). The CIMEL sun-photometer is part of the AErosol Robotics NETwork (AERONET) which is currently located at over 500 ground sites worldwide. It is used to collect ground based AOD data. The multi-channel CIMEL sun-photometer, automatic Sun, and sky scanning radiometer, only measure direct solar irradiance and sky radiance at the Earth's surface during daylight hours (Sun above the horizon) after the cloud screening and quality control and processing. The lack of data and the different number of observations during the month is sometimes due to instruments not working properly, and during the monsoon (July-August) the availability of data depends on rain. Therefore, due to rain or clouds obscuring the sun, the number of observations is reduced during these periods.

The optical properties of aerosol particles over Jaipur have been studied using level 2 AERONET monthly data. The AOD is available via AERONET at numerous wavelengths between 340 and 1640 nm, with a precision of * ± 0.01 at 440 nm and * ±0.02 at lesser wavelengths [16]. The prevalent aerosol type was determined using the AERONET aerosol products, such as Angstrom Exponent (AE), based on the 440 nm and 870 nm wavelengths [60].

The Version 2.0 AERONET retrieval products are expanded and improved by providing total estimated errors (systematic, random, and bias) for the radiometric and microphysical inversion products. The Level 2 data, upgraded annually and only accessible for a portion of the campaign, will be utilized for a sensitivity study. These data include pre-field, and post-field calibration applied, automatically cleared clouds, and manually examined data. The calibration uncertainty is the primary source of the estimated 0.01-0.02 uncertainty in AOD (Level 2) [54]. In India, the AERONET program of NASA, USA, has erected a CIMEL sun/sky radiometer at several locations. The processing algorithms have advanced from Version 1.0 to Version 2.0 to Version 3.0. The AERONET and PHOTONS websites both offer access to the Version 3.0 databases. Version 3.0 AOD data are computed for three levels of data quality: Level 1.0 (unscreened), Level 1.5 (cloud-screened and quality regulated), and Level 2.0 (quality-assured) [61]. Version 3.0 and Level 2 data were the only ones widely accessible for all the parameters, thus we used them in our investigation. Others have used this level data in the past, and the level 1.5 AOD value's departure from level 2.0 is found to be between 0 and 5% over IGB [62]. Previous studies have described the data processing, cloud screened and the quality confirmed and inversion methods [11, 16, 54, 60, 61].

3. Results and Discussion

3.1. Annual and Monthly Variation of AOD and Angstrom Exponent (AE) over the Study Region from April-2009 to December-2017

Fig. 2(A) shows the monthly variations of average aerosol optical depth at 500 nm, 440 nm, and 340 nm. Fig. 2(B) shows the Angstrom exponent (AE) at 440 – 870 nm, 500-870 nm, and 340 – 440 nm over Jaipur from April-2009 to December-2017.

The peak value of aerosol optical depth at AOD 500 nm was 0.78 ± 0.25, AOD 440 nm 0.85 ± 0.27, and AOD 300 nm 1.00 ± 0.30 in July-2011 and the minimum value at AOD 500 nm was 0.27 ± 0.13, AOD 440 nm 0.30 ± 0.14, and AOD 300 nm was 0.37 ± 0.17 in March 2013. The higher AOD_{500} nm, AOD_{440} nm, AOD_{340} nm values in June and July could be due to higher quantities of water vapor in the atmosphere due to higher precipitation levels in these months. This may be caused by the large amounts of water vapor and sea salts transported throughout India from the Arabian Sea and Bay of Bengal, primarily from the Indian Ocean [63]. Since water vapor and AOD are connected, greater water vapor concentrations also result in higher concentrations of AOD because water vapor-soluble aerosols grow hygroscopically in their presence [64]. Long-range dust transport from the Arabian Peninsula also contributes to net regional aerosol loading, with AOD over the northern Arabian Sea increasing significantly in May–June compared to April [65].

The Angstrom exponent (AE) is a characteristic parameter of AOD wavelength dependence that shows the size of aerosol particles. Depending upon the size aerosols particle categories in four types, particle size: fine mode ($d < 2.5\ \mu m$) and coarse mode ($d > 2.5\ \mu m$); fine mode is divided on the nuclei mode (about $0.005\ \mu m < d < 0.1\ \mu m$) and accumulation mode ($0.1\mu m < d < 2.5\ \mu m$). Particles in the coarse mode are associated to primary emissions from things like burning biomass and industrial processes. This kind of particle strongly correlates with changes in mass concentration [66, 67]. Most fine-mode particles are considered secondary aerosols produced by gaseous precursors, oxidants, and/or changes in the weather [68-74]. Coarse-mode particles are quite small and increase with decreasing particle size (fine-mode). Fig. 2(B) depicts the temporal variation of AE over Jaipur.

AE data were retrieved for the period 2009–2017 from AERONET. Fig. 2(B) describes in contrast to the variance in AOD_{500} nm, AOD_{440} nm, and AOD_{340} nm values, September had the highest monthly average Angstrom Exponent (AE) was maximum (1.53 ± 0.43) for 500 – 870 nm, (1.49 ± 0.4) for 440-870 nm and (1.19 ± 0.32) for 340 – 440 nm wavelengths in September 2011 respectively. The lowest value of Angstrom Exponent (AE) recorded (0.26 ± 0.12) for 340 – 440 nm, (0.16 ± 0.08) for 440 – 870 nm and

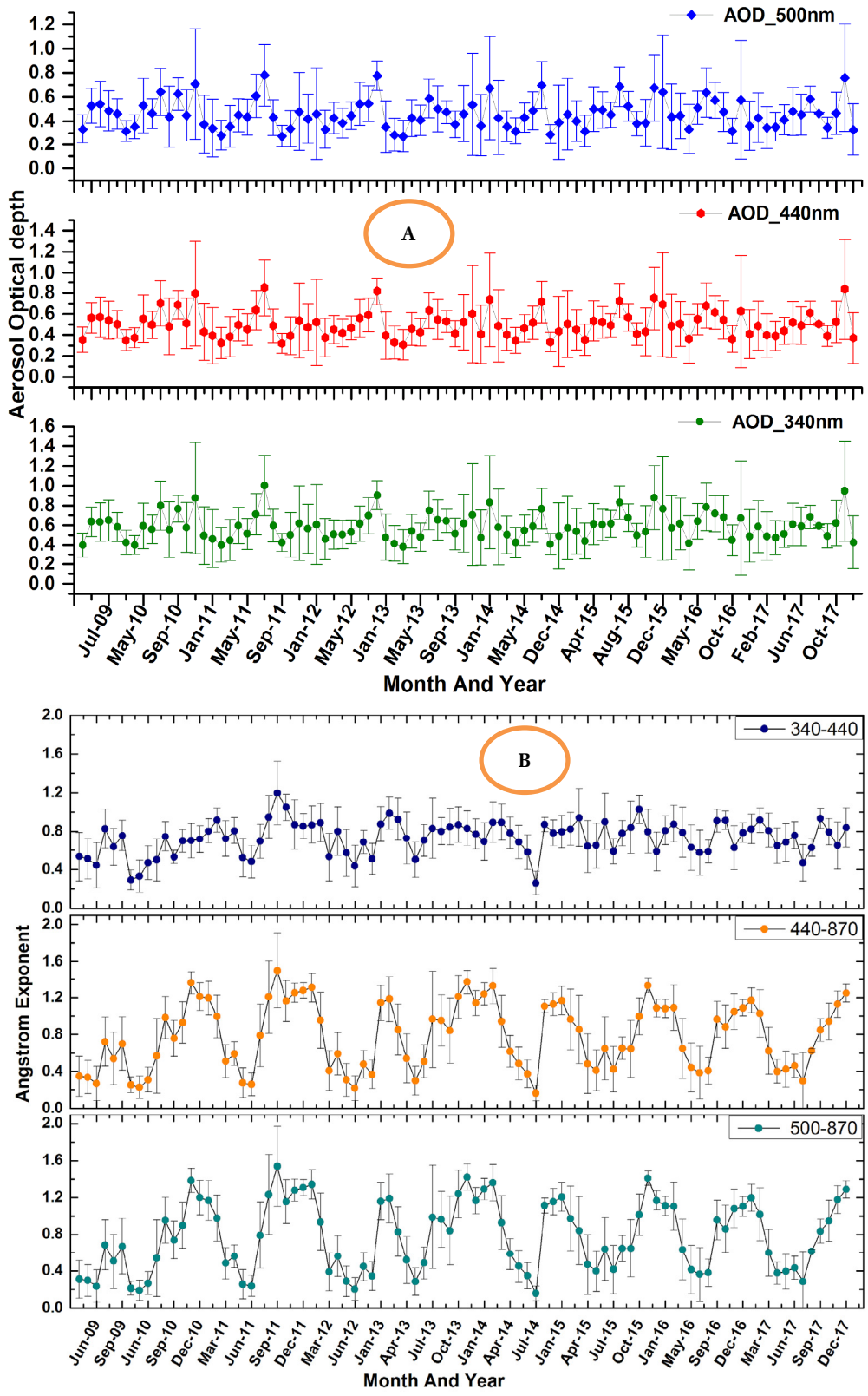

Fig. 2. (A) Aerosols Optical Depth (AOD) and (B) Angstrom Exponent (AE annual variations with mean ± Standard Deviation for wavelengths (500-870 nm,440-870 nm, and 340-440 nm) at Jaipur station from April-2009 to December-2017.

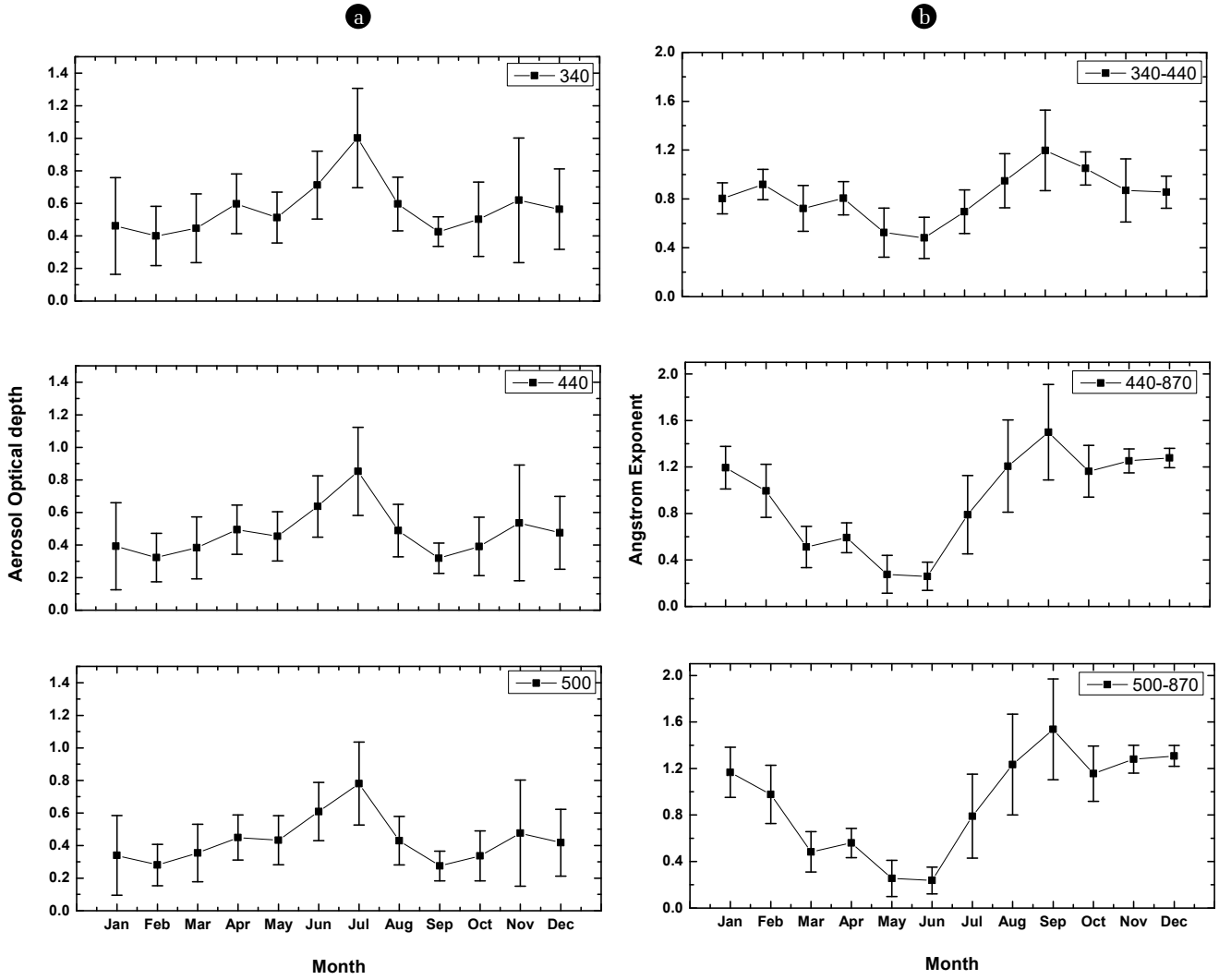

Fig. 3. Monthly variations with mean ± SD in the (A) AOD_{500} nm, AOD_{440} nm, and AOD_{340} nm and (B) Angstrom Exponent (500-870 nm, 440-870 nm, and 340-440 nm) at Jaipur station.

(0.15 ± 0.07) for 500 – 870 nm wavelengths and during June 2014 respectively showing the dominance of course particles as shown in Fig. 2(B). The higher value of the Angstrom Exponent denotes the preponderance of fine-mode particles with more significant spectral variation in AOD.

Fig. 3 shows the inter-comparisons of the annual cycle of mean AOD variation for different months in mean ± SD values of AOD_{500} nm, AOD_{440} nm, AOD_{340} nm and Angstrom Exponent 500 – 870 nm, 440 – 870 nm, and 340 – 440 nm at Jaipur station during 2011. For a better understanding of the AOD trend over the region, 2011 year is being selected because of the availability of the data points throughout the year. It is clear from the results that the AOD (Fig. 3(A)) values were higher in July and lower values for wavelength 340 nm, then gradually decreased with an increase in wavelengths, while these Angstrom Exponent (AE) values were found to be higher in September lower in June month for all wavelengths. Then from July, these values were found to increase till December (Fig. 3(B)). Because the extinction's spectral structure is associated with the particle size, the Angstrom Exponent (AE) is also a significant predictor of the most prominent aerosol sizes [54-56].

3.2. Seasonal Variation of AOD and AE at Different Wavelengths

The seasonal average AOD values at 340 nm, 440 nm, and 500 nm at the Jaipur station during the study period April-2009 to December-2017 are shown in Fig. 4(A). The mean highest, ± Standard Deviation values of AOD_{340} nm, AOD_{440} nm, and AOD_{500} nm were 0.57±0.10, 0.62±0.10, and 0.73±0.11, respectively observed in Monsoon. However, the lowest AOD values observed during Pore-Monsoon for AOD_{340} nm, AOD_{440} nm, and AOD_{500} nm were 0.44±0.06, 0.47±0.06, and 0.55±0.08, respectively. Aerosols can absorb moisture and grow hygroscopically, which favors the formation of particles such as sulfate, nitrate, sea-salt,

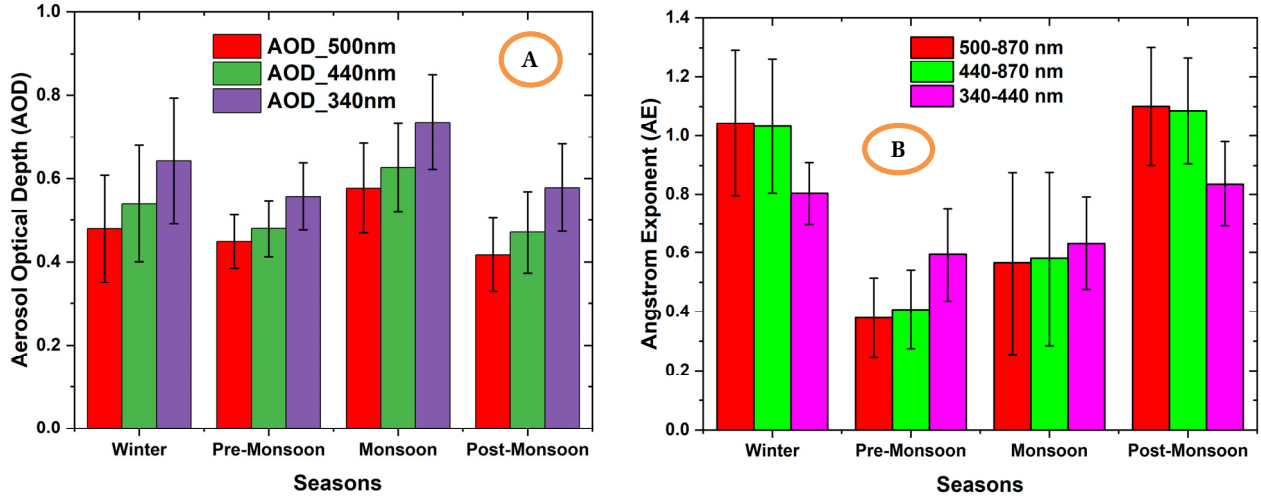

Fig. 4. (A) Aerosol Optical Depth (AOD) and (B) Angstrom Exponent (AE) seasonal variations with mean ± Standard Deviation for wavelengths (500-870 nm,440-870 nm and 340-440 nm) at Jaipur station during April-2009 to December-2017.

or mineral dust particles [75-77]. It is demonstrating from Fig. 5(A) that the values of AOD fluctuate at shorter wavelengths (340 nm and 440 nm) differ from that at longer wavelengths (500 nm) at Jaipur station.

The seasonal variations of average Angstrom Exponent (AE) values at 500 – 870 nm, 440 – 870 nm, and 340 – 440 nm at the Jaipur station during the study period April-2009 to December-2017 are shown in Fig. 4(B). The mean ± SD values of Angstrom Exponent 500 – 870 nm, 440 – 870 nm, and 340 – 440 nm were 1.10±0.20, 1.08±0.17, and 0.83±0.14, respectively observed highest in post-Monsoon. However, the lowest AE values observed during Pre-monsoon for Angstrom Exponent 500 – 870 nm, 440 – 870 nm, and 340 – 440 nm were 0.37±0.13, 0.40±0.14, and 0.59±0.15, respectively. The Angstrom Exponent (AE) is found to be minimal during the Pre-monsoon month of April-May, and it gradually increases to the maximum values during the post-Monsoon period (December and March).

3.3. Backward Trajectories Analysis Using HYSPLIT Model

In terms of altitude and distance, the backward trajectories indicate the many long-range transport modes. The backward trajectories of air masses are necessary to determine the origin of aerosol sources and the transport paths that lead to observation sites. Over Jaipur during the pre-monsoon season, the air mass appears to have traveled from distant source areas, including the Arabian Peninsula, the Sahara Desert, and the Thar Desert. Almost identical sources of aerosols over IGP were reported [22]. The Middle East and the Thar Desert regions are the principal sources of the contaminated dust particles that dominate the air masses over Jaipur [78]. 5-day back trajectories from the HYSPLIT model at 500, 1000, and 1500 m altitudes were undertaken to identify the sources and analyze how transport patterns affect the concentrations of air pollutants over Jaipur, India (Fig. 5). The day with highest (>1) values of AOD were selected for Jaipur region during the study period. The back trajectories during 1 November 2010, 1 June 2012, 8 November 2013, 1 January 2015, 1 October 2016 and 19 November 2017 were studied over Jaipur based on the National Oceanic and Atmospheric Administration's Hybrid Single-Particle Lagrangian Integrated Trajectories (HYSPLIT) model (https://www.ready.noaa.gov/HYSPLIT.php) [79].

Fig. 5 depicts the travel pathway and origin of dust particles with 120-h back trajectories simulated for three distinct heights (500, 1000, and 1500 m AMSL) at 08:00 UTC over Jaipur using the NOAA HYSPLIT trajectory model. The air mass at low and middle altitudes comes from the continental region, as seen in (Fig. 5). From January to December, the air mass appears to be transported from distant source regions such as the Arabian Peninsula, the Sahara Desert, and the Thar Desert over Jaipur. The variations in the two parameters (i.e., AOD and AE) over Jaipur are almost gradual and stable, notwithstanding natural changes or fluctuations in meteorological conditions and aerosol transport. Different kinds of aerosols could be transported from various regions to the observation sites due to changes in seasonal wind patterns. Examples include sea salt from the ocean, dust from the desert, and anthropogenic aerosols from biomass and urban-industrial sources. Except in the instance of July and December 2011, where the air mass at higher altitudes appears to originate from The Persian and The Oman gulf region, the air mass trajectories unambiguously indicate the Thar Desert as the main source of the dust. Gautam *et al.* [22] identified essentially the same sources of aerosols over IGP. According to Tiwari *et al.* [80], the air masses dominant over Jaipur are polluted dust particles primarily from the Middle East and the Thar Desert regions. As the pre-monsoon month's progress, coarser particles like dust and sea salt become increasingly articulated with longer pathways and significant latitudinal variations, causing havoc on Jaipur [62].

3.4. Classification of Aerosol Types Using Cluster Techniques (AOD Versus AE)

The daily scatter graph of AOD 500 nm versus The Angstrom Exponent (AE) (440-870 nm) over Jaipur during April 2009-

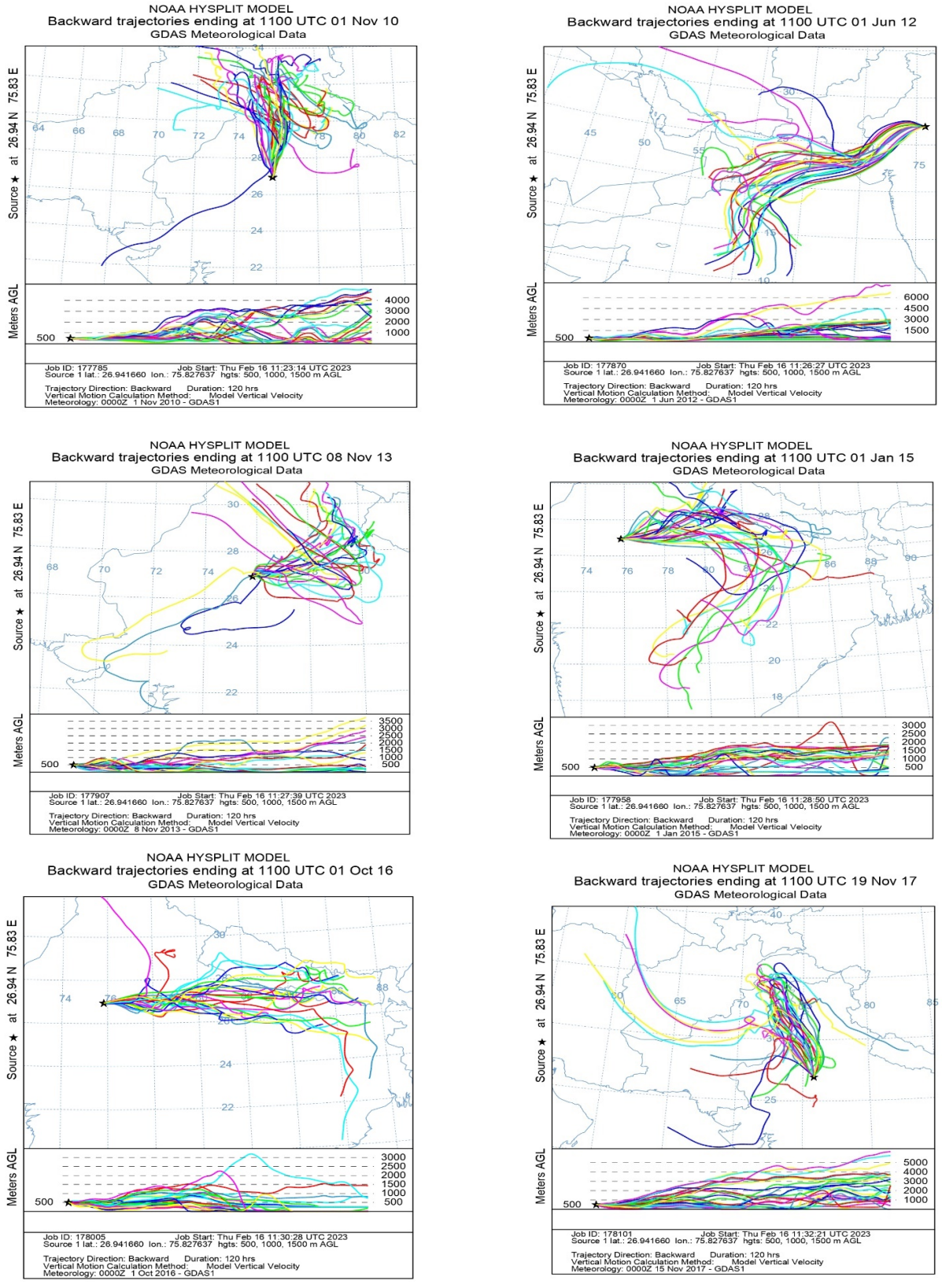

Fig. 5. HYSPLIT model Five-day back trajectories on specific days when the recorded AOD is maximum over (Jaipur region).

December 2017 illustrates in (Fig. 6). The cluster technique is useful to categorize and evaluate the impacts of various sources on the daily aerosol concentration and aerosol particle size. The variation in the relationship between the AOD and The Angstrom Exponent (AE) [13,81–85] is also being investigated. The atmospheric Aerosol can be categorized accordingly by using different methods. Correlation between AOD and Angstrom Exponent (AE) is one of the most efficient method to determine size and amount of different atmospheric particles [81–83]. AOD calculates the reduction of solar radiation due to aerosol-induced sunlight scattering and absorption. The Angstrom formula calculates how the AOD depends on wavelength. By identifying physically comprehensible cluster locations, this scatter plot can be used to differentiate between the various forms of aerosol [83]. For greater consistency in identifying aerosols, the multi-cluster analysis is significantly more effective than pairings of clusters (as in the current study) [86]. Aerosols can be characterized mostly using Mahalanobis classification which is a practical technique of merging many dimensions of multi-wavelength optical information [84].

Several researchers classified different aerosol types using the AOD-AE clustering method across various regions [83, 87]. AOD > 0.25 and AE < 0.7 indicate coarse mode particles, such as dust, and were used as threshold values to identify different aerosols

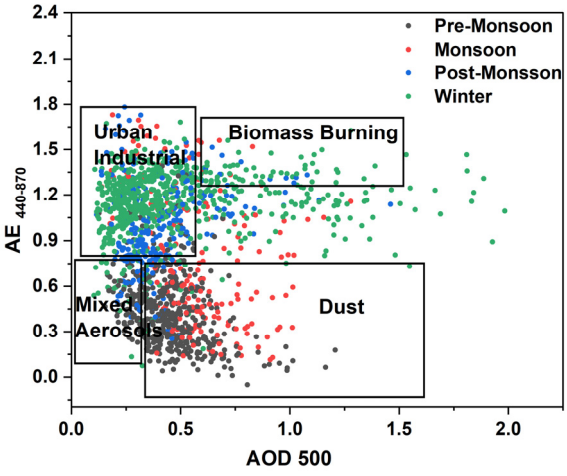

Fig. 6. Daily scattered plot of AOD (500 nm) versus AE (440-870) over Jaipur station during April-2009 to December-2017.

[86]. Mixed aerosols were shown by 0.01 < AOD < 0.7 and 0.7 < AE < 1.7 [88]. Urban/industrial aerosols were distinguished using 1.7 < AOD > 0.01 and 1.7 < AE > 0.7 [81]. Urban and industrial aerosols were present throughout the year over the research location. AOD > 0.5 and AE > 1.0, on the other hand, indicate biomass-burning aerosols are present over the selected region [88].

4. Conclusions

The present study demonstrates the significant variations in atmospheric parameters over the Jaipur region. The study mainly emphasizes trends in Aerosols Optical Depth (AOD) and Angstrom Exponent (AE) over the Jaipur in the vicinity of the dust source northwestern part of India during April-2009 to December-2017. The characteristics of aerosol optical properties were observed using CIMEL sun-photometer instruments, which is part of the AErosol Robotics NETwork (AERONET). The atmospheric pollutants are responsible for the monthly, annual, and seasonal variations. Among the several sources, the presence of anthropogenic dust affects the studied region dominantly. Based on the relationship between AOD and AE, the various aerosol types were categorized which confirm the presence of different aerosol particles over the Jaipur region. Additionally, it helps to calculate the radiation budget and its effects on Earth's climate. Hence, the accessibility of more geographic ground-based measurements and aerosols identification are of utmost significance.

It is crucial to emphasize the unpredictability, constraints, and potential outcomes of current investigation. Within certain bounds, the HYSPLIT model can give a crucial overview of the pollutant transit routes to the target area. In a present study, ground data and aerosol dispersion models may be utilized to better understand the aerosol properties over the Jaipur region, which are close to the Indo-Gangetic Plan (IGP).

The following points were concluded from the present study.

- The monthly AOD and AE variation trend significantly changes throughout the study period over the study location. Higher AOD values were observed during July-2011, while lower AOD values were observed during March-2013 for 340 nm, 440 nm, and 500 nm wavelengths, respectively. The average AE shows higher values in September 2011 and the lowest observed

Table 1. AOD (500 nm) versus AE (440-870) over different Indian stations with aerosol types.

Study Region	Types of Aerosols	AOD (500 nm)	AE	References
Hyderabad	Urban/Industrial	AOD > 0.50	$AE_{380-870}$ < 1.0	Kaskaoutis *et al.* (2009) [82]
	Desert Dust	AOD > 0.60	$AE_{380-870}$ < 0.70	
Dibrugarh	Continental Average	AOD > 0.20	$AE_{380-1225}$ < 1.4	Pathak *et al.* (2012) [89]
	Desert Dust	AOD > 0.45	$AE_{380-1225}$ < 0.7	
Jaipur	dust	AOD > 0.25	$AE_{440-870}$ < 0.7	Present Study
	Mixed aerosols	AOD < 0.3	$AE_{440-870}$ < 0.7	
	Urban/Industrial	0.01< AOD < 0.7	$AE_{440-870}$ 0.7 < AE < 1.7	
	biomass burning	A AOD > 0.5	$AE_{440-870}$ > 1.0	

value in July 2014 for all wavelengths. Lack of soil moisture raises the production rate of natural aerosols such as soil dust and they are not removed from the atmosphere by rainfall. This could be the reason for high aerosols optical depth values during June and July onwards.

- Seasonal fraction of AOD trend observed higher AOD for wavelengths 340 nm as compared to 440 nm, and 500 nm wavelengths, while the opposite trend was observed for AE during seasonal analysis.
- During the pre-monsoon season, Middle Eastern countries, the Sahara Desert, and India's Thar Desert, have been identified as significant sources of transported mineral dust and pollutants over the study region.
- In order to determine the origin of air masses in the Western Indian (Jaipur) region, the HYSPLIT model was employed for trajectory analysis. Apart from regional and local sources (such as biomass combustion, resuspended desert dust, vehicle, and industrial pollution), incremental increase was seen throughout the investigation.
- The 5-day air mass back trajectory analysis also shows that the western (arid) regions of Iraq, Afghanistan, Iran, and Pakistan are foremost contributors of atmospheric aerosols and the mineral dust during the pre-monsoon and monsoon. As well as study shows the urban industrial and dust particles are the major source of aerosols loading over the study region.

Acknowledgments

We gratefully acknowledge and thank the AERONET group for making all the data available in the form of Level 2.0 quality assured product after necessary screening and post calibrations. The authors thank the NOAA Air Resources Laboratory (ARL) for the provision of the HYSPLIT transport and dispersion model and website http://www.arl.noaa.gov/ready.php used in this publication. We are also thankful to NASA for meteorological data, "These data were obtained from the NASA Langley Research Center (LaRC) POWER Project funded through the NASA Earth Science/Applied Science Program." (https://power.larc.nasa.gov/).

Author Contributions

R.S. (PhD student) has done the formal analysis, investigation, methodology, and writing original draft. K.P. (Professor) has done the conceptualization, review, editing and supervision.

Conflict-of-Interests

The authors declare that they have no conflict of interest.

References

1. Charlson RJ, Schwartz SE, Hales JM, Cess RD, Coakley Jr JA, Hansen JE, *et al*. Climate forcing by anthropogenic aerosols. *Science* 1992;255:423–30. https://doi.org/10.1126/science.
2. Haywood J, Boucher O. Estimates of the direct and indirect radiative forcing due to tropospheric aerosols: A review. *Rev. Geo.* 2000;38:513–43. https://doi.org/10.1029/1999RG000078.
3. Liu X, Gu J, Li Y, Cheng Y, Qu Y, Han T, *et al*. Increase of aerosol scattering by hygroscopic growth: Observation, modeling, and implications on visibility. *Atm. Res.* 2013;132:91–101. https://doi.org/10.1016/j.atmosres.2013.04.007.
4. Mahowald N. Aerosol indirect effect on biogeochemical cycles and climate. *Science* 2011;334:794–6. https://doi.org/10.1126/science.1207374.
5. Myhre G. Consistency between satellite-derived and modeled estimates of the direct aerosol effect. *Science* 2009;325:187–90. http:// doi.org/ 10.1126/science.1174461.
6. Eck TF, Holben BN, Dubovik O, Smirnov A, Goloub P, Chen HB, *et al*. Columnar aerosol optical properties at AERONET sites in central eastern Asia and aerosol transport to the tropical mid-Pacific. *J. Geophys. Res.* 110, D06202. https://doi.org/10.1029/2004JD005274.
7. AR5 Climate Change 2013: The Physical Science Basis — IPCC n.d. https://www.ipcc.ch/report/ar5/wg1/ (accessed July 6, 2022).
8. Obregón MA, Serrano A, Cancillo ML, Cachorro VE, Toledano C. Aerosol radiometric properties at Western Spain (Cáceres station). *Int. J. Clim.* 2015;35:981–90. D06202, https://doi.org/10.1029/2004JD005274.
9. Panicker AS, Lee DI, Kumkar YV, Kim D, Maki M, Uyeda H. Decadal climatological trends of aerosol optical parameters over three different environments in South Korea. *Int. J. Clim.* 2013;33:1909–16. https://doi.org/10.1002/joc.3557.
10. Kaufman YJ, Tanré D, Boucher O. A satellite view of aerosols in the climate system. *Nature* 2002;419:215–23. https://doi.org/10.1038/nature01091.
11. Holben BN, Tanre D, Smirnov A, Eck TF, Slutsker I, Abuhassan N, *et al*. An emerging ground-based aerosol climatology: Aerosol optical depth from AERONET. *J. Geophys. Res.* 2001; 106:12067–97. https://doi.org/10.1029/2001JD900014.
12. Dubovik O, Holben B, Eck TF, Smirnov A, Kaufman YJ, King MD, *et al*. Variability of absorption and optical properties of key aerosol types observed in worldwide locations. *J. Atm. Sci.* 2002;59:590–608. https://doi.org/10.1175/1520-0469(2002).
13. Russell PB, Bergstrom RW, Shinozuka Y, Clarke AD, DeCarlo PF, Jimenez JL, *et al*. Absorption Angstrom Exponent in AERONET and related data as an indicator of aerosol composition. *Atm. Chem. Phy.* 2010;10:1155–69. https://doi.org/10.5194/acp-10-1155-2010.
14. Giles DM, Holben BN, Eck TF, Sinyuk A, Smirnov A, Slutsker I, *et al*. An analysis of AERONET aerosol absorption properties and classifications representative of aerosol source regions. *J. Geophys. Res.* 2012;117. https://doi.org/10.1029/2012JD018127.
15. Kim D-H, Sohn B-J, Nakajima T, Takamura T, Takemura T, Choi B-C, *et al*. Aerosol optical properties over East Asia determined from ground-based sky radiation measurements. *J. Geophys. Res.* 2004;109. https://doi.org/10.1029/2003JD003387.
16. Holben BN, Eck TF, Slutsker I al, Tanre D, Buis JP, Setzer A, *et al*. AERONET—A federated instrument network and data

archive for aerosol characterization. *Rem. Sens. Env.* 1998;66:1–16. https://doi.org/10.1016/S0034-4257(98)00031-5.
17. Singh RP, Dey S, Tripathi SN, Tare V, Holben B. Variability of aerosol parameters over Kanpur, northern India. *J. Geophys. Res.* **109,** 2004;109. https://doi.org/10.1029/2004JD004966.
18. Dey S, Tripathi SN, Singh RP, Holben BN. Influence of dust storms on the aerosol optical properties over the Indo-Gangetic basin. *J. Geophys. Res.* 2004;109. https://doi.org/10.1029/2004JD004924.
19. Pant P al, Hegde P, Dumka UC, Sagar R, Satheesh SK, Moorthy KK, *et al*. Aerosol characteristics at a high-altitude location in central Himalayas: Optical properties and radiative forcing. *J. Geophys. Res.* 2006;111. https://doi.org/10.1029/2005JD006768.
20. Beegum SN, Moorthy KK, Nair VS, Babu SS, Satheesh SK, Vinoj V, *et al*. Characteristics of spectral aerosol optical depths over India during ICARB. *J. Earth. Syst. Sci.* 2008;117:303–13. https://doi.org/10.1007/s12040-008-0033-y.
21. Pandithurai G, Dipu S, Dani KK, Tiwari S, Bisht DS, Devara PCS, *et al*. Aerosol radiative forcing during dust events over New Delhi, India. *J. Geophys. Res.* 2008;113. https://doi.org/10.1029/2008JD009804.
22. Gautam R, Hsu NC, Lau K-M. Premonsoon aerosol characterization and radiative effects over the Indo-Gangetic Plains: Implications for regional climate warming. *J. Geophys. Res.* 2010;115. https://doi.org/10.1029/2010JD013819.
23. Gautam R, Hsu NC, Lau K-M, Tsay S-C, Kafatos M. Enhanced pre-monsoon warming over the Himalayan-Gangetic region from 1979 to 2007: ENHANCED HIMALAYAN WARMING. *Geo. Res. Lett.* 2009;36: L07704. https://doi.org/10.1029/2009GL037641.
24. Soni K, Singh S, Bano T, Tanwar RS, Nath S, Arya BC. Variations in single scattering albedo and Angstrom absorption exponent during different seasons at Delhi, India. *Atmo. Environ.* 2010;44:4355–63. https://doi.org/10.1016/j.atmosenv.2010.07.058.
25. Bonasoni P, Laj P, Marinoni A, Sprenger M, Angelini F, Arduini J, *et al*. Atmospheric Brown Clouds in the Himalayas: first two years of continuous observations at the Nepal Climate Observatory-Pyramid(5079m). *Atmos. Chem. Phys.* 2010;10:7515–31. https://doi.org/10.5194/acp-10-7515-2010.
26. Decesari S, Facchini MC, Carbone C, Giulianelli L, Rinaldi M, Finessi E, *et al*. Chemical composition of PM 10 and PM 1 at the high-altitude Himalayan station Nepal Climate Observatory-Pyramid (NCO-P) (5079 m asl). *Atmos. Chem. Phys*. 2010;10:4583–96. https://doi.org/10.5194/acp-10-4583-2010.
27. Gobbi GP, Angelini F, Bonasoni P, Verza GP, Marinoni A, Barnaba F. Sunphotometry of the 2006–2007 aerosol optical/radiative properties at the Himalayan Nepal Climate Observatory-Pyramid (5079 m asl). *Atmos. Chem. Phys.* 2010;10:11209–21. https://doi.org/10.5194/acp-10-11209-2010.
28. Ram K, Sarin MM, Hegde P. Long-term record of aerosol optical properties and chemical composition from a high-altitude site (Manora Peak) in Central Himalaya. *Atmos. Chem. Phys.* 2010;10:11791–803. https://doi.org/10.5194/acp-10-11791-2010.
29. Kumar S, Kumar S, Kaskaoutis DG, Singh RP, Singh RK, Mishra AK, *et al*. Meteorological, atmospheric, and climatic perturbations during major dust storms over Indo-Gangetic Basin. *Aeolian. Res.* 2015;17:15–31. https://doi.org/10.1016/j.aeolia.2015.01.006.
30. Kaskaoutis DG, Sinha PR, Vinoj V, Kosmopoulos PG, Tripathi SN, Misra A, *et al*. Aerosol properties and radiative forcing over Kanpur during severe aerosol loading conditions. *Atmos. Environ.* 2013;79:7–19. https://doi.org/10.1016/j.atmosenv.2013.06.020.
31. Prasad AK, Singh RP. Changes in aerosol parameters during major dust storm events (2001-2005) over the Indo-Gangetic Plains using AERONET and MODIS data. *J. Geophys. Res.* 2007;112. https://doi.org/10.1029/2006JD007778.
32. Prakash D, Payra S, Verma S, Soni M. Aerosol particle behavior during Dust Storm and Diwali over an urban location in north western India. *Nat. Hazards.* 2013;69:1767–79. https://doi.org/10.1007/s11069-013-0780-1.
33. Verma S, Payra S, Gautam R, Prakash D, Soni M, Holben B, *et al*. Dust events and their influence on aerosol optical properties over Jaipur in Northwestern India. *Environ. Monit. Assess.* 2013;185:7327–42. https://doi.org/10.1007/s10661-013-3103-9.
34. Lawrence MG, Lelieveld J. Atmospheric pollutant outflow from southern Asia: a review. *Atmos. Chem. Phys.* 2010;10:11017–96. https://doi.org/10.5194/acp-10-11017-2010.
35. Chinnam N, Dey S, Tripathi SN, Sharma M. Dust events in Kanpur, northern India: Chemical evidence for source and implications to radiative forcing. *Geophys. Res. Lett.* 2006;33. https://doi.org/10.1029/2005GL025278.
36. Nair VS, Moorthy KK, Alappattu DP, Kunhikrishnan PK, George S, Nair PR, *et al*. Wintertime aerosol characteristics over the Indo-Gangetic Plain (IGP): Impacts of local boundary layer processes band long-range transport. *J. Geophys. Res.* 2007;112. https://doi.org/10.1029/2006JD008099.
37. Prospero JM, Ginoux P, Torres O, Nicholson SE, Gill TE. Environmental characterization of global sources of atmospheric soil dust identified with the Nimbus 7 Total Ozone Mapping Spectrometer (TOMS) absorbing aerosol product. *Rev. Geophys.* 2002;40:2–1. https://doi.org/10.1029/2000RG000095.
38. Washington R, Todd M, Middleton NJ, Goudie AS. Dust-storm source areas determined by the total ozone monitoring spectrometer and surface observations. *Ann. Assoc. Am. Geogr.* 2003; 93:297–313. https://doi.org/10.1111/1467-8306.9302003
39. Pease PP, Tchakerian VP, Tindale NW. Aerosols over the Arabian Sea: geochemistry and source areas for aeolian desert dust. *J. Arid. Environ.* 1998;39:477–96. https://doi.org/10.1006/jare.1997.0368.
40. Léon J-F, Legrand M. Mineral dust sources in the surroundings of the north Indian Ocean. *Geophys. Res. Lett.* 2003;30. https://doi.org/10.1029/2002GL016690.
41. Lau KM, Kim MK, Kim KM. Asian summer monsoon anomalies induced by aerosol direct forcing: the role of the Tibetan *Plateau. Clim. Dyn.* 2006;26:855–64. https://doi.org/10.1007/s00382-006-0114-z.
42. Meehl GA, Arblaster JM, Collins WD. Effects of black carbon aerosols on the Indian monsoon. *J. Clim.* 2008;21:2869–82.

https://doi.org/10.1175/2007JCLI1777.1.
43. Wang C, Kim D, Ekman AM, Barth MC, Rasch PJ. Impact of anthropogenic aerosols on Indian summer monsoon. *Geophys. Res. Lett.* 2009;36. https://doi.org/10.1029/2009GL040114.
44. Gautam R, Hsu NC, Lau K-M, Tsay S-C, Kafatos M. Enhanced pre-monsoon warming over the Himalayan-Gangetic region from 1979 to 2007. *Geophys. Res. Lett.* 2009;36. https://doi.org/10.1029/2009GL037641.
45. Sharma SK, Mandal TK. Chemical composition of fine mode particulate matter (PM2. 5) in an urban area of Delhi, India and its source apportionment. *Urban Clim.* 2017;21:106–22. https://doi.org/10.1016/j.uclim.2017.05.009.
46. Sharma D, Singh M, Singh D. Impact of post-harvest biomass burning on aerosol characteristics and radiative forcing over Patiala, north-west region of India. *J. Eng. Res.* 2011;8:11–24. https://doi.org/10.3126/jie.v8i3.5927.
47. Kaskaoutis DG, Kumar S, Sharma D, Singh RP, Kharol SK, Sharma M, *et al*. Effects of crop residue burning on aerosol properties, plume characteristics, and long-range transport over northern India. *J. Geophys. Res. Atmos.* 2014;119:5424–44. https://doi.org/10.1002/2013JD021357.
48. Hansen J, Fung I, Lacis A, Rind D, Lebedeff S, Ruedy R, *et al*. Global climate changes as forecast by Goddard Institute for Space Studies three-dimensional model. *J. Geophys. Res. Atmos.* 1988;93:9341–64. https://doi.org/10.1029/JD093iD08p09341.
49. Dammann KW, Hollmann R, Stuhlmann R. Study of aerosol impact on the earth radiation budget with satellite data. *Adv. Space Res.* 2002;29:1753–7.https://doi.org/10.1016/S0273-1177(02)00106-0.
50. Kanakidou M, Seinfeld JH, Pandis SN, Barnes I, Dentener FJ, Facchini MC, *et al*. Organic aerosol and global climate modelling: a review. *Atmos. Chem. Phys.* 2005;5:1053–123. https://doi.org/10.5194/acp-5-1053-2005.
51. Von Schneidemesser E, Monks PS, Allan JD, Bruhwiler L, Forster P, Fowler D, *et al*. Chemistry and the linkages between air quality and climate change. *Chem. Rev.* 2015;115:3856–97. https://doi.org/10.1021/acs.chemrev.5b00089.
52. Vanos JK, Cakmak S, Kalkstein LS, Yagouti A. Association of weather and air pollution interactions on daily mortality in 12 Canadian cities. *Air Qual. Atmos. Health* 2015;8:307–20. https://doi.org/10.1007/s11869-014-0266-7.
53. Dhaka SK, Kumar V, Panwar V, Dimri AP, Singh N, Patra PK, *et al*. PM2. 5 diminution and haze events over Delhi during the COVID-19 lockdown period: an interplay between the baseline pollution and meteorology. *Sci. Rep.* 2020;10:13442. https://doi.org/10.1038/s41598-020-70179-8.
54. Eck TF, Holben BN, Reid JS, Dubovik O, Smirnov A, O'neill NT, *et al*. Wavelength dependence of the optical depth of biomass burning, urban, and desert dust aerosols. *J. Geophys. Res. Atmos.* 1999;104:31333–49. https://doi.org/ 10.1029/1999JD900923.
55. Cachorro VE, Durán P, Vergaz R, de Frutos AM. Columnar physical and radiative properties of atmospheric aerosols in north central Spain. *J. Geophys. Res. Atmos.* 2000;105:7161–75. https://doi.org/10.1029/1999JD901165.
56. Schuster GL, Dubovik O, Holben BN. Angstrom exponent and bimodal aerosol size distributions. *J. Geophys. Res. Atmos.* 2006;111. https://doi.org/10.1029/2005JD006328.
57. Sikka DR. Desert Climate and Its Dynamics. *Current Science* 1997:72:35–46. http://www.jstor.org/stable/24098628.
58. Soni M, Payra S, Sinha P, Verma S. A performance evaluation of WRF model using different physical parameterization scheme during winter season over a semi-arid region, India. *Int. J. Earth Sci.* 2014;1:104–14.
59. Payra S, Soni M, Kumar A, Prakash D, Verma S. Intercomparison of aerosol optical thickness derived from MODIS and in situ ground datasets over Jaipur, a semi-arid zone in India. *Environ. Sci. Technol.* 2015;49:9237–46. https://doi.org/10.1021/acs.est.5b02225.
60. Dubovik O, King MD. A flexible inversion algorithm for retrieval of aerosol optical properties from Sun and sky radiance measurements. *J. Geophys. Res. Atmos.* 2000;105:20673–96. https://doi.org/10.1029/2000JD900282.
61. Smirnov A, Holben BN, Eck TF, Dubovik O, Slutsker I. Cloud-screening and quality control algorithms for the AERONET database. *Remote Sens. Environ.* 2000;73:337–49. https://doi.org/10.1016/S0034-4257(00)00109-7.
62. Tiwari S, Srivastava AK, Singh AK. Heterogeneity in pre-monsoon aerosol characteristics over the Indo-Gangetic Basin. *Atmos. Environ.* 2013;77:738–47. https://doi.org/10.1016/j.atmosenv.2013.05.035.
63. Mamun MI, Islam M, Mondol PK. The Seasonal Variability of Aerosol Optical Depth over Bangladesh Based on Satellite Data and HYSPLIT Model. *American J. Remote Sens.* 2014;2:20. https://doi.org/10.11648/j.ajrs.20140204.11.
64. Alam K, Iqbal MJ, Blaschke T, Qureshi S, Khan G. Monitoring spatio-temporal variations in aerosols and aerosol–cloud interactions over Pakistan using MODIS data. *Adv. Space Res.* 2010;46:1162–76. https://doi.org/10.1016/j.asr.2010.06.025.
65. Badarinath KVS, Kharol SK, Kaskaoutis DG, Sharma AR, Ramaswamy V, Kambezidis HD. Long-range transport of dust aerosols over the Arabian Sea and Indian region—A case study using satellite data and ground-based measurements. *Glob. Planet. Change.* 2010;72:164–81. https://doi.org/10.1016/j.gloplacha.2010.02.003.
66. Han T, Xu W, Chen C, Liu X, Wang Q, Li J, *et al*. Chemical apportionment of aerosol optical properties during the Asia-Pacific Economic Cooperation summit in Beijing, China. *J. Geophys. Res. Atmos.* 2015;120:12,281-12,295. https://doi.org/10.1002/2015JD023918.
67. Kajino M, Deushi M, Sekiyama TT, Oshima N, Yumimoto K, Tanaka TY, *et al*. NHM-Chem, the Japan meteorological agency's regional meteorology – chemistry model: Model evaluations toward the consistent predictions of the chemical, physical, and optical properties of aerosols. *J. Meteorol. Soc. Jpn. Ser II* 2019;97:337–74. https://doi.org/10.2151/jmsj.2019-020.
68. Kitamori Y, Mochida M, Kawamura K. Assessment of the aerosol water content in urban atmospheric particles by the hygroscopic growth measurements in Sapporo, Japan. *Atmos. Environ.* 2009;43:3416–23. https://doi.org/10.1016/j.atmosenv.2009.03.037.
69. Cheng Y-H, Li Y-S. Influences of traffic emissions and meteoro-

logical conditions on ambient pm10 and pm2.5 levels at a highway toll station. *Aerosol Air Qual. Res.* 2010;10:456–62. https://doi.org/10.4209/aaqr.2010.04.0025.
70. Xue J, Griffith SM, Yu X, Lau AKH, Yu JZ. Effect of nitrate and sulfate relative abundance in PM2.5 on liquid water content explored through half-hourly observations of inorganic soluble aerosols at a polluted receptor site. *Atmos. Environ.* 2014;99:24–31. https://doi.org/10.1016/j.atmosenv.2014.09.049.
71. Mesquita SR, Dachs J, van Drooge BL, Castro-Jiménez J, Navarro-Martín L, Barata C, *et al*. Toxicity assessment of atmospheric particulate matter in the Mediterranean and Black Seas open waters. *Sci. Total Environ.* 2016;545–546:163–70. https://doi.org/10.1016/j.scitotenv.2015.12.055.
72. Tan H, Cai M, Fan Q, Liu L, Li F, Chan PW, *et al*. An analysis of aerosol liquid water content and related impact factors in Pearl River Delta. *Sci. Total Environ.* 2017;579:1822–30. https://doi.org/10.1016/j.scitotenv.2016.11.167.
73. Kong L, Du C, Zhanzakova A, Cheng T, Yang X, Wang L, *et al*. Trends in heterogeneous aqueous reaction in continuous haze episodes in suburban Shanghai: An in-depth case study. *Sci. Total Environ.* 2018;634:1192–204. https://doi.org/10.1016/j.scitotenv.2018.04.086.
74. Kudo S, Iijima A, Kumagai K, Tago H, Ichijo M. An exhaustive classification for the seasonal variation of organic peaks in the atmospheric fine particles obtained by a gas chromatography/mass spectrometry. *Environ. Technol. Innov.* 2018;12:14–26. https://doi.org/10.1016/j.eti.2018.04.011.
75. Yan P, Pan X, Tang J, Zhou X, Zhang R, Zeng L. Hygroscopic growth of aerosol scattering coefficient: A comparative analysis between urban and suburban sites at winter in Beijing. *Particuology.* 2009;7:52–60. https://doi.org/10.1016/j.partic.2008.11.009.
76. Bian H, Chin M, Rodriguez JM, Yu H, Penner JE, Strahan S. Sensitivity of aerosol optical thickness and aerosol direct radiative effect to relative humidity. *Atmos. Chem. Phys.* 2009;9:2375–86. https://doi.org/10.5194/acp-9-2375-2009.
77. Li WJ, Shao LY, Buseck PR. Haze types in Beijing and the influence of agricultural biomass burning. *Atmos. Chem. Phys.* 2010;10:8119–30. https://doi.org/10.5194/acp-10-8119-2010.
78. Tiwari S, Singh AK. Variability of aerosol parameters derived from ground and satellite measurements over Varanasi located in the Indo-Gangetic Basin. *Aerosol Air Qual. Res.* 2013;13:627–38. https://doi.org/10.4209/aaqr.2012.06.0162.
79. Draxler RR, Rolph GD. HYSPLIT (HYbrid Single-Particle Lagrangian Integrated Trajectory) model access via NOAA ARL READY, NOAA Air Resources Laboratory. *Silver Spring, MD* 2010;25. Available from: http://ready.arl.noaa.gov/HYSPLIT.Php.
80. Tiwari S, Srivastava AK, Singh AK, Singh S. Identification of aerosol types over Indo-Gangetic Basin: implications to optical properties and associated radiative forcing. *Environ. Sci. Pollut. Res.* 2015;22:12246–60. https://doi.org/10.1007/s11356-015-4495-6.
81. Bibi H, Alam K, Bibi S. In-depth discrimination of aerosol types using multiple clustering techniques over four locations in Indo-Gangetic plains. *Atmos. Res.* 2016;181:106–114. https://doi.org/10.1016/j.atmosres.2016.06.017.
82. Kaskaoutis DG, Badarinath KVS, Kumar Kharol S, Rani Sharma A, Kambezidis HD. Variations in the aerosol optical properties and types over the tropical urban site of Hyderabad, India. *J. Geophys. Res. Atmos.* 2009;114. https://doi.org/10.1029/2009JD012423.
83. Kaskaoutis DG, Kumar Kharol S, Sinha PR, Singh RP, Kambezidis HD, Rani Sharma A, *et al*. Extremely large anthropogenic-aerosol contribution to total aerosol load over the Bay of Bengal during winter season. *Atmos. Chem. Phys.* 2011;11:7097–117. https://doi.org/10.5194/acp-11-7097-2011.
84. Burton SP, Ferrare RA, Hostetler CA, Hair JW, Rogers RR, Obland MD, *et al*. Aerosol classification using airborne High Spectral Resolution Lidar measurements–methodology and examples. *Atmos. Meas. Tech.* 2012;5:73–98. https://doi.org/10.5194/amt-5-73-2012.
85. Wang Z, Liu D, Wang Z, Wang Y, Khatri P, Zhou J, *et al*. Seasonal characteristics of aerosol optical properties at the SKYNET Hefei site (31.90 N, 117.17 E) from 2007 to 2013. *J. Geophys. Res. Atmos.* 2014;119:6128–39. https://doi.org/10.1002/2014JD021500.
86. Kedia S, Ramachandran S, Holben BN, Tripathi SN. Quantification of aerosol type, and sources of aerosols over the Indo-Gangetic Plain. *Atmos. Environ.* 2014;98:607–19. https://doi.org/10.1016/j.atmosenv.2014.09.022.
87. Kumar KR, Sivakumar V, Reddy RR, Gopal KR, Adesina AJ. Identification and classification of different aerosol types over a subtropical rural site in Mpumalanga, South Africa: Seasonal variations as retrieved from the AERONET Sunphotometer. *Aerosol Air Qual. Res.* 2014;14:108–23. https://doi.org/10.4209/aaqr.2013.03.0079.
88. Sharma M, Kaskaoutis DG, Singh RP, Singh S. Seasonal variability of atmospheric aerosol parameters over Greater Noida using ground sunphotometer observations. *Aerosol Air Qual. Res.* 2014;14:608–22. https://doi.org/10.4209/aaqr.2013.06.0219.
89. Pathak B, Bhuyan PK, Gogoi M, Bhuyan K. Seasonal heterogeneity in aerosol types over Dibrugarh-North-Eastern India. *Atmos. Environ.* 2012;47:307–15. https://doi.org/10.1016/j.atmosenv.2011.10.061.